

Article

Recovery of Lead (II) Ions from Aqueous Solutions Using G-26 and MTS9570 Resins with Sulfonic/Phosphonic Functional Groups

Salem Elfeghe ¹, Qiuyue Sheng ^{1,2}, Abbas Mamudu ¹, Lesley Anne James ¹  and Yahui Zhang ^{1,*} 

¹ Department of Process Engineering, Faculty of Engineering and Applied Science, Memorial University of Newfoundland, St. John's, NL A1B 3X5, Canada

² School of Resources and Civil Engineering, Northeastern University, Shenyang 110819, China

* Correspondence: yahuiz@mun.ca

Abstract: This study presents Pb(II) recovery/removal from water solutions using two different commercial ion-exchange resins, i.e., Dowex G-26 with sulfonic functional group and Puromet™ MTS9570 with sulfonic and phosphonic functional groups. Overall, 100% Pb(II) recovery/removal by both resins was obtained at solution pH 3.5, resin dosage 25 g/L, adsorption time 30 min, room temperature, and initial Pb(II) concentration 1000 mg/L. Langmuir, Freundlich, and Temkin isotherms were used to model the experimental data. The mechanism of the adsorption process was investigated using kinetic and thermodynamic models. The experimental data fitted very well with the pseudo-second-order kinetic model, and thermodynamic analysis showed that the adsorption of Pb(II) from acidic solution onto both resins was a spontaneous and endothermic process in nature. Regeneration of the resins loaded with lead ions was tested for three cycles to evaluate the resin recyclability. Good stability of G-26 and performance degradation of MTS9570 resin was observed.

Keywords: Pb(II); ion-exchange resins; regeneration; isotherms; kinetics; thermodynamics



Citation: Elfeghe, S.; Sheng, Q.; Mamudu, A.; James, L.A.; Zhang, Y. Recovery of Lead (II) Ions from Aqueous Solutions Using G-26 and MTS9570 Resins with Sulfonic/Phosphonic Functional Groups. *Minerals* **2022**, *12*, 1312. <https://doi.org/10.3390/min12101312>

Academic Editors: Mostafa Benzaazoua and Yassine Taha

Received: 10 September 2022

Accepted: 14 October 2022

Published: 18 October 2022

Publisher's Note: MDPI stays neutral with regard to jurisdictional claims in published maps and institutional affiliations.



Copyright: © 2022 by the authors. Licensee MDPI, Basel, Switzerland. This article is an open access article distributed under the terms and conditions of the Creative Commons Attribution (CC BY) license (<https://creativecommons.org/licenses/by/4.0/>).

1. Introduction

With more demands for modern industrial products, heavy-metals consumption is widely increased in many fields. Their environmental impacts bring up serious concern because of their toxicity and non-degradability. Exposure to these pollutants can be harmful to human and environmental species [1–4]. Lead is one of the toxic metals and is discharged from different industrial activities such as mining, metals production, battery industry, and fuels combustion [5–7]. Lead's existence in water recourses can cause different diseases such as hepatitis and anemia [8–11]. According to the World Health Organization (WHO) guideline 2017, the maximum acceptable concentration for lead in drinking water is 0.01 mg/L [12–14]. Therefore, lead removal from wastewaters has become an important task, which also has the benefit of lead metal recovery.

Several remediation techniques have been used for lead recovery/removal from wastewater, such as chemical precipitation, electrodialysis, electrolysis, reverse osmosis, adsorption, and ion exchange [15–19]. Among these technologies, resin adsorption is one of the most suitable methods for the removal of lead and other toxic metals from aqueous solution due to its low cost, process simplicity, low remnant metal concentration, and high efficiency.

Various resins with different functional groups such as strong acid cation (SAC) resins with sulfonic acid group (-SO₃H), including Amberlite IR-120, Dowex 50W, Purolite C100, Lewatit SP-112, D-001, 732-CR, Dowex 50WX8, Amberjet 1200 Na, and C 160; weak acid cation (WAC) resins with carboxylic acid group (-COOH) such as Amberlite IRC-50/IRC-86, Lewatit CNP 80, and Purolite C-104; weak acid and chelating resins with iminodiacetic acid groups such as Purolite S-930, Amberlite IRC 718, and Lewatit TP 207; and acid and

chelating resins with amino-phosphonic groups such as Purolite S-940 and Purolite S-950 were studied for lead removal from aqueous solutions [20–23].

Qian et al. [24] studied the kinetics and thermodynamics of lead removal from aqueous solution using 732 cation-exchange resin with sulfonic acid group in hydrogen type in the temperature range of 298–328 K and Pb(II) concentration range of 5–50 mol/m³. The experimental results show that the adsorption isotherm data agreed closely with the Langmuir isotherm and the maximum monolayer exchange for Pb(II) was 484.0 mg/g at 308 K. Thermodynamic studies demonstrate that the adsorption of Pb(II) onto 732-CR is spontaneous and exothermic in nature. This resin was also tested by Guo et al. for removing lead from aqueous solutions [25]. The maximum sorption capacity of Pb(II) at pH 4.0 was 396.8 mg/g resin from their study. Tabatabaei et al. [26] investigated removal of lead from aqueous system using Amberlite IR-120 with sulfonic acid group and compared its efficiency with natural zeolite.

Vergili et al. [27] investigated the performance of WAC resin Lewatit CNP80 with carboxylic (-COOH) functional group for Pb(II) removal from battery industry wastewater. The Pb(II) removal efficiency in batch experiments was found to be 83.3% at 25 °C, with resin dosage of 2 g/L in 6 h contact time. The Pb(II) removal efficiency could increase slightly from 83% to 87% with increase in temperature. A similar study was reported by Xiong and Yao using resin (110-H) with carboxylic group for Pb(II) adsorption in HAc-NaAc medium, obtaining the maximum lead adsorption capacity of 485 mg/g at pH 6.7 and 298 K [28].

Thu et al. [29] synthesized thiol-functionalized mesoporous silicas by co-condensation of tetraethoxysilane and varying contents of 3-mercaptopropyltrimethoxysilane in acidic medium with the block copolymer Pluronic 123 as a structure directing agent. Adsorption of lead from water by the thiol-functionalized silicas was studied. The maximum adsorption capacity was 0.19 mmol Pb per gram of adsorbent at 90 min contact time with initial Pb(II) concentration 200 mg/L and temperature 30 °C. The adsorption efficiency of the lead-reloaded sample can reach 80% after five cycles of adsorption-elution compared with the fresh ones.

Removal of lead using Purolite S-930 resin with iminodiacetic functional group in aqueous solution was studied by Merganpour et al. [30]. The column adsorption results concluded that 91.12% of mean lead removal ratio from drinking water containing up to 22 µg/L Pb can be achieved using Purolite S-930 during 21-day service at pH 6.5, which demonstrates an economic and technically feasible lead-removal process.

Ren et al. [31] reported a comparison study of Pb(II) adsorption on XC-72 carbon black and multi-walled carbon nanotubes (MWCNTs). The load of Pb(II) was 125.0 mg/g and 17.5 mg/g on XC-72 and MWCNTs, respectively, at pH 6.0 and 293 K temperature.

The performance of G-26 and MTS9570 resins have been examined by us for removing Cd(II) ions successfully from acidic solutions. Maximum cadmium-removal rates of 99.2% and 98.9% were achieved for G-26 and MTS9570, respectively, at 30 min of adsorption, 5.0 of initial solution pH, 1000 mg/L of initial metal concentration, and 0.01 g/mL of resin dosage for G-26 and 0.025 g/mL of resin dosage for MTS9570 [32,33]. As lead and cadmium are both persistent bio-accumulative toxic (PBT) metals, and they often coexist in nature, comparative study of G-26 and MTS9570 for Pb(II) removal from aqueous solution was conducted in this work for a co-removal process in the future. The research involves exploratory experiments using twenty-three resins with different functional groups. The adsorption process using G-26 and MTS9570 was evaluated with adsorption isotherms, kinetic, and thermodynamic studies at different operation conditions.

2. Experimental Details

2.1. Materials

All the chemicals used to prepare Pb(II) solutions were of analytical reagent grade. Commercial synthetic resins Dowex G-26 in hydrogen form and Puromet™ MTS9570 were supplied by DuPont™ and Purolite US, respectively. Lead nitrate Pb(NO₃)₂ (obtained

from A&C American Chemicals Ltd., Montreal, Canada) was used to prepare 1000 mg/L stock standard solution. The working standard solutions were prepared by the dilution of appropriate volumes of the stock standard solution with deionized water. Solution pH was adjusted with 0.1 mol/L HCl or 1% NaOH solutions. The properties of the resins are given in Table 1.

Table 1. Physical and chemical properties of resins [32].

Characteristics	G-26	MTS9570
Matrix	Styrene-DVB	Polystyrene-DVB
Ionic form as shipped	H ⁺ form	H ⁺ form
Functional group	Sulfonic	Phosphonic and sulfonic
Appearance	Uniform particle size	Spherical beads
Structure	gel	Macroporous
Capacity	2.0 eq/L	18 g/L eq/L
Bed size	0.65 mm ± 0.05	0.315–0.850 mm
Uniformity coefficient	1.1	1.4
Water retention	45%–52%	55%–70%
Specific gravity	1.22 g/mL	1.12 g/mL

2.2. Apparatus

Instruments used in this study were as follows: Inductively coupled plasma (ICP) spectroscopy was used for metal concentration analysis; an electric shaker (model Promax 2020, Heidolph Instruments GmbH & Co. KG, Schwabach, Germany) was used for adsorption tests with 20 mL solutions in 125 mL flasks. The solution pH was measured with a pH meter (model Orion Star A211).

2.3. Experimental Procedure

2.3.1. Activation of Resins

Before experiments, resins were initially washed in DI water at 150 rpm on a reciprocating platform shaker for 1 h. Then, they were activated with a solution of 10% (*v/v*) HCl and agitated at 150 rpm for 24 h. Subsequently, the resins were washed two times in DI water at 150 rpm for 1 h and dried at room temperature for 7 days. The dried resins were stored in dry bottles and were used for future experiments.

2.3.2. Adsorption Tests

A standard solution of lead (1000 ppm) was prepared by dissolving a weighed amount of lead nitrate salt in distilled water, and the pH was adjusted by adding 0.1 mol/L HCl. The adsorption performances of G-26 and MTS 9570 for Pb(II) ions were investigated by batch experiments at different temperatures. Batch adsorption experiments were conducted at a constant volume of 20 mL metal ions solution and using different doses of dry resins, i.e., from 0.1 to 0.5 g/L. The adsorption behavior of metal ions by the adsorbents was studied in the pH range of 1.5–5.5. Samples of metal solution and resins in 125 mL flasks were shaken in an electric shaker at different contact times ranging from 5 to 180 min and at the fixed speed of 150 rpm. After reaching the equilibrium stage, the solution was filtered and analyzed with XRF. The batch adsorption experiments were performed in triplicate and adopted the average value. The errors of the measurements were within 10%. The adsorption capacities of G-26 and MTS9570 exchangers and the removal percentage of Pb(II) were calculated using the following Equations (1) and (2), respectively.

$$Q = \frac{(C_o - C_e)V/1000}{M} \quad (1)$$

$$\text{and \% removal of Pb (II) ions} = \frac{(C_i - C_o)}{C_i} \times 100 \quad (2)$$

where Q is the adsorption capacity in mg/g at time t ; C_i , C_o , and C_e are the initial, final, and equilibrium concentrations of Pb(II) in mg/L, respectively; V is the volume of Pb (II) solution in mL, and M is the total amount of resin in grams (g).

3. Results and Discussion

3.1. Exploration of Pb Recovery/Removal Using Resins

There are many commercial resins available from different manufacturing companies. These resins have different chemical and physical properties. To explore the suitable resin for Pb(II) uptake, twenty-three resins were tested, which have different functional groups. The exploration process was conducted at resin amounts ranging from 0.1 g to 0.5 g at 20 mL constant volume metal solution, 180 min adsorption time, 150 adsorption speed, 1000 mg/L solution concentration, pH 3.5, and 20 ± 1 °C room temperature.

Figure 1 illustrates fourteen resins that have a Pb(II)-removal percentage above or close to 90%. These resins mainly contain sulfonic, phosphonic/sulfonic, amino/phosphonic, iminodisatic, bis-picolylamine, or sulfonic/trimethylamine group(s), while the other nine resins with functional group(s) of iso-thiouonium, carboxylic, N-methylglucamine, diethylhexylphosphate (D2EHPA), thiourea, aminomethylphosphonic, or trimethyl ammonium have relatively low adsorption performance for lead ions (Figure 2). Among the twenty-three resins tested, Dowex G-26 resin with sulfonic group and Purolite MTS 9570 resin with phosphonic/sulfonic groups were selected. These two resins have been tested by the same author, and they had high efficiency for removal of cadmium and copper as well [32].

3.2. Effect of Adsorption Time

A series of adsorption time tests for lead recovery/removal were carried out with the initial metal concentration of 1000 mg/L, resin dose 0.5 g, and shaking speed 150 rpm at pH 3.5 and room temperature. The removal percentage of adsorbed lead (II) ions onto both resins increased with time, as shown in Figure 3. It can be found that the adsorption time necessary to reach equilibrium was within 30 min. Further increase in time had no effect on the adsorption of lead for both exchangers. The uptake percentage for Pb(II) increased from 49.3% to 100% and from 45.8% to 100% for G-26 and MTS9570, respectively. Further, 30 min adsorption time was adopted for subsequent tests.

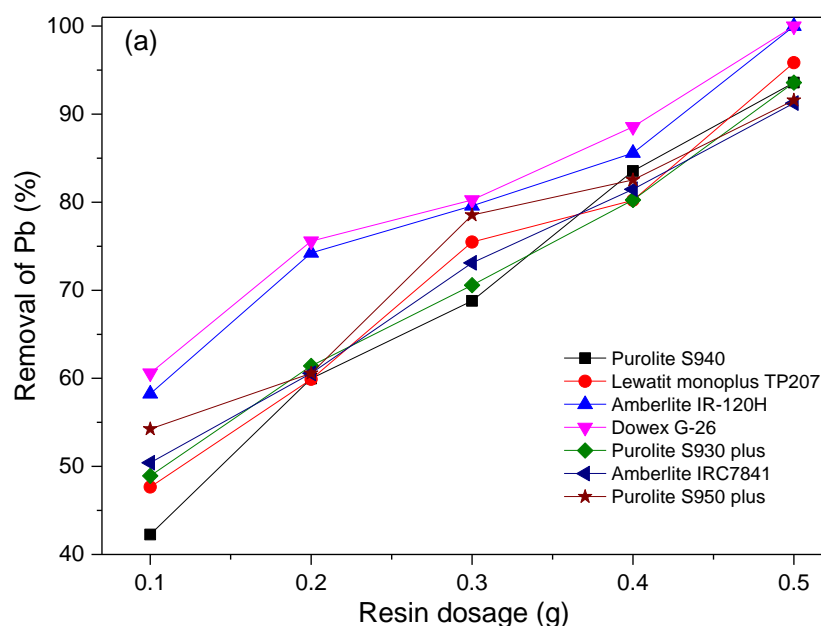


Figure 1. Cont.

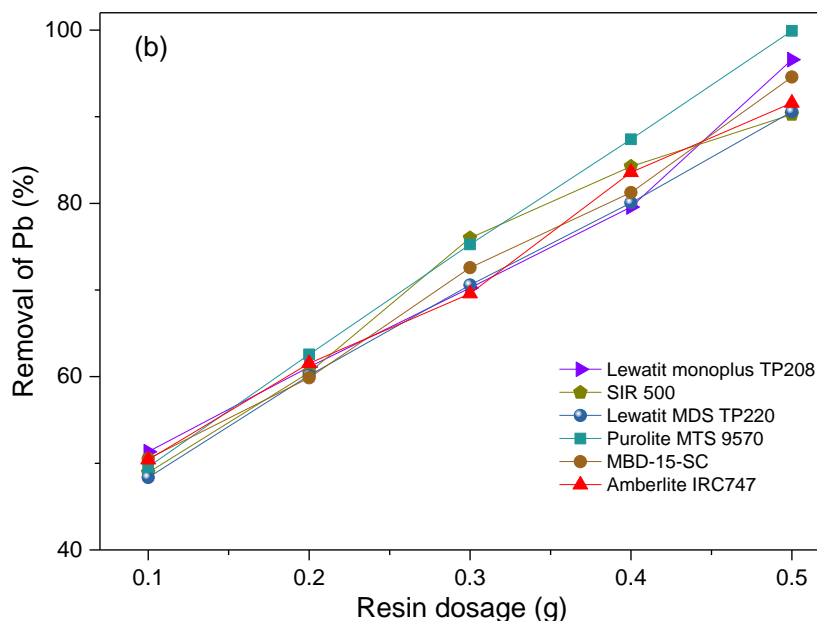


Figure 1. Resins with high removal rate of Pb (II) at 30 min contact time, 150 rpm agitation speed, 20 mL volume, pH 4.5, concentration 1000 mg/L, and temperature 20 °C. (a) Purolite S940, Lewatit monopulus TP207, Amberlite IR-120H, Dowex G-26, Purolite S930 plus, Amberlite IRC7841, and Purolite S950 plus resin. (b) Lewatit monopulus TP208, SIR 500, Lewatit MDS TP220, Purolite WTS 9570, MBD-15-SC, and Amberlite IRC747 resin.

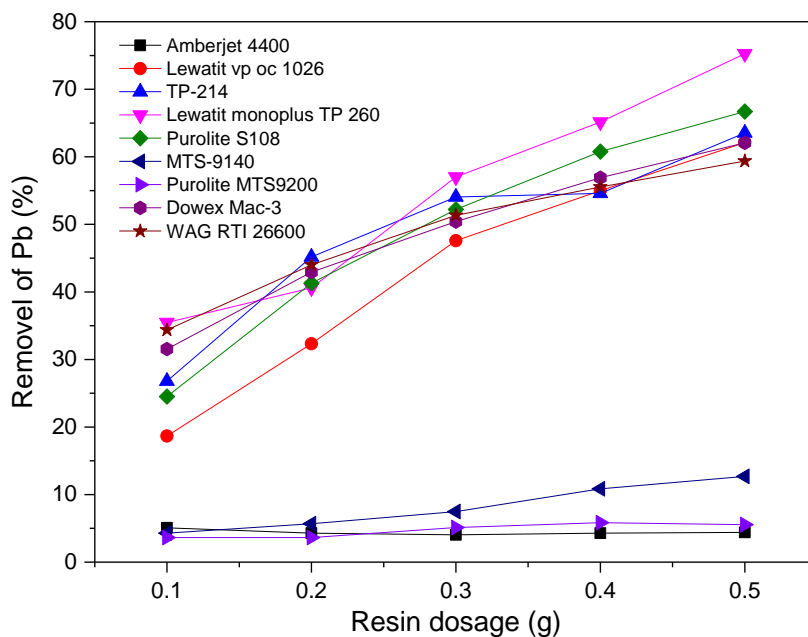


Figure 2. Resins with low removal rate of Pb (II) at 30 min contact time, 150 rpm agitation speed, 20 mL volume, pH 4.5, concentration 1000 mg/L, and temperature 20 °C.

3.3. Effect of Adsorbent Dosage

Figure 4 presents the removal of Pb(II) by G-26 and MTS9570 as a function of resin dosage. Resin dosage was varied from 5 to 30 g/L, while other conditions were the same as in the adsorption time tests. Increasing resin dosage increased the removal percentage of Pb(II). When the resin dosage increased to 25 g/L, Pb(II)-removal rates were close to 100% for both resins. This indicates that both resins can be used as adsorbents to remove Pb(II) ions effectively, and 25 g/L resin dosage was used for subsequent tests.

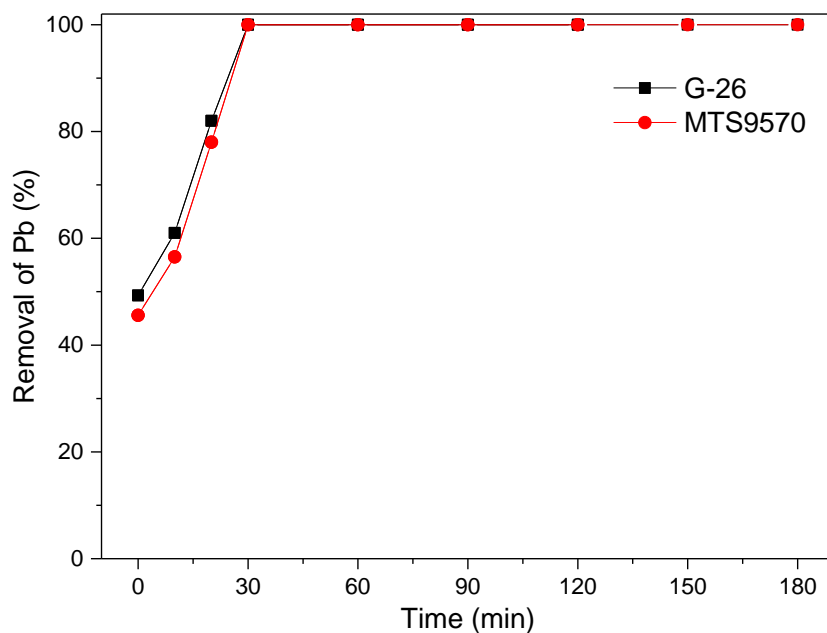


Figure 3. Effect of agitation time on adsorption of Pb(II) using G-26 and MTS9570 exchange resins at 0.5 g of resin dosage, 30 min contact time, 150 rpm agitation speed, pH 3.5, concentration 1000 mg/L, and temperature 20 °C.

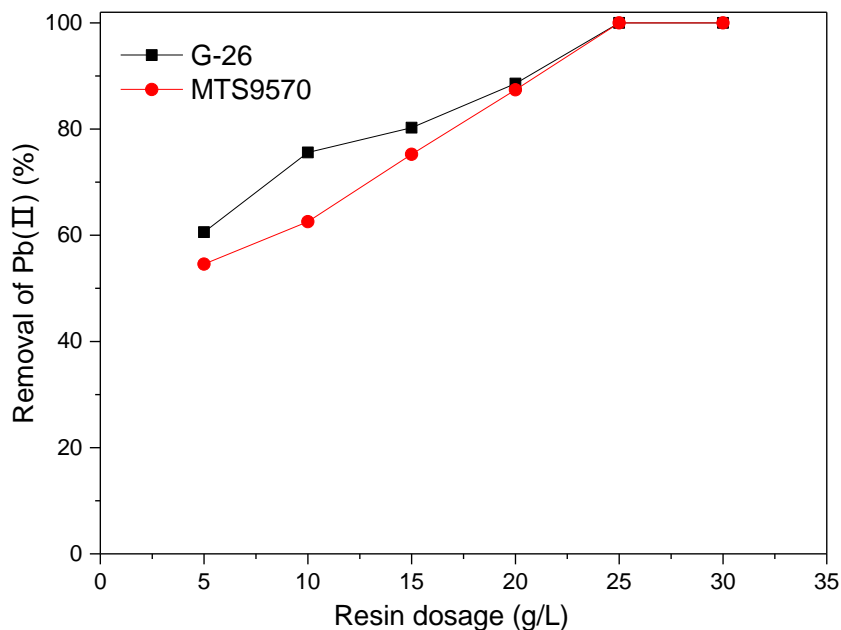


Figure 4. Effect of resin dosage on adsorption of Pb(II) using G-26 and MTS9570 exchange resins at 30 min contact time, 150 rpm agitation speed, pH 3.5, concentration 1000 mg/L, and temperature 20 °C.

3.4. Effect of pH

The influence of pH on the removal of Pb(II) was investigated at pH range 1.5–5.5, while other conditions were the same as in the adsorbent dosage tests. As seen from Figure 5, pH does not have a significant effect on the adsorption of Pb(II) onto G-26 resin in the entire explored pH range (1.5–5.5). The removal rate of Pb(II) was slightly low at pH 1.5 for MTS9570. Precipitation of lead was observed at pH > 5.5. Therefore, in the subsequent experiments, the solution pH was kept at 3.5.

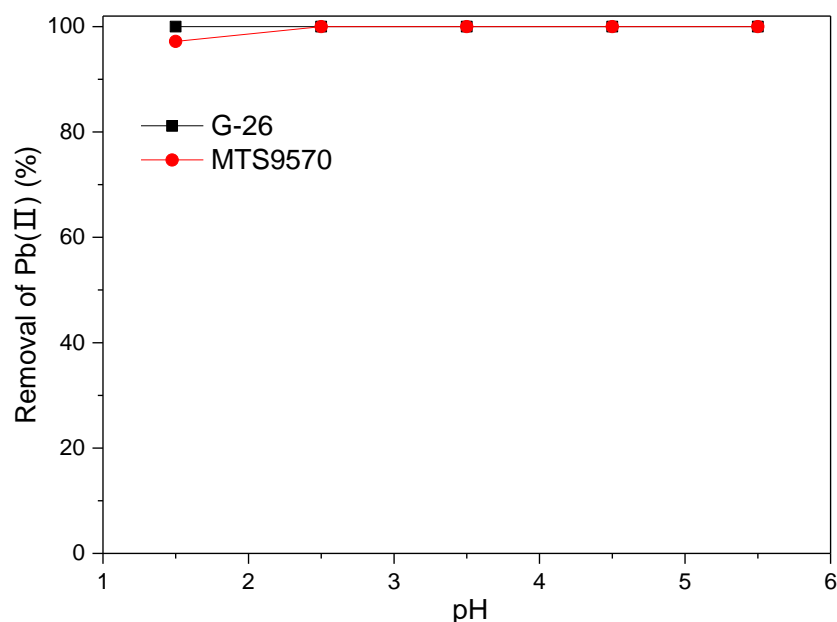


Figure 5. Effect of pH on adsorption of Pb(II) using G-26 and MTS9570 exchange resins at 0.5 g of resin dosage, 30 min contact time, 150 rpm agitation speed, concentration 1000 mg/L, and temperature 20 °C.

3.5. Effect of Temperature

Adsorption experiments were conducted at four different temperatures (20, 40, 60, and 80 °C) to study the performance of the selected resins on the adsorption of lead ions. As shown in Figure 6, the removal percentage of Pb(II) increased with the rising temperature, which indicates that the adsorption of Pb(II) ions onto G-26 and MTS9570 resins is endothermic in nature.

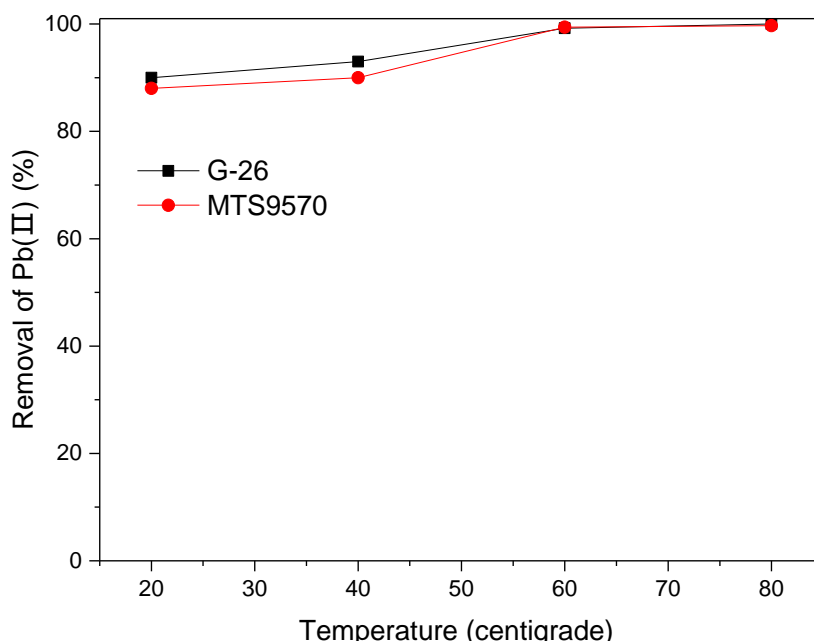


Figure 6. Effect of temperature on adsorption of Pb(II) using G-26 and MTS9570 resins at 0.5 g of resin dosage, 30 min contact time, 150 rpm agitation speed, pH 3.5, and concentration 1000 mg/L.

3.6. Effect of Initial Metal Ion Concentration

Effect of initial metal concentration on Pb(II) adsorption onto G-26 and MTS9570 resins was explored at 20 °C (shown in Figure 7). The removal percentages of lead on the two

resins are both close to 100% in the Pb concentration range of 100–1000 mg/L. At the high metal concentration of 1200 mg/L, the removal percentage of Pb decreased, which is due to less availability of favorable sites for adsorption on the resin beads. The result obtained in this work is consistent to the results reported by Al Anber et al. [34] and Elfeghe et al. [32].

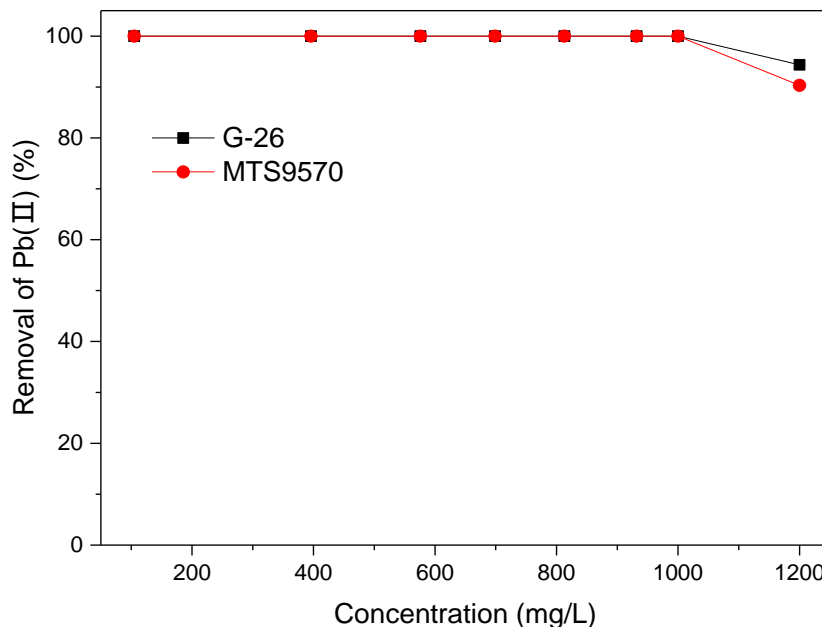


Figure 7. Effect of initial metal concentration on adsorption of Pb(II) onto G-26 and MTS9570 resins at 0.5 g of resin dosage, 30 min contact time, 150 rpm agitation speed, pH 3.5, and temperature 20 °C.

3.7. Adsorption Isotherms

The sorption isotherms play an important role in the design of adsorption systems. Three popular isotherm models, i.e., Langmuir [35], Freundlich [36], and Temkin [37] isotherms, were applied for the equilibrium modelling of Pb(II) adsorption on the resins.

The Langmuir isotherm is commonly used to describe monolayer sorption at equilibrium, and the linear form is given by the following equation:

$$\frac{C_e}{q_e} = \frac{1}{Q^0 b} + \frac{C_0}{Q^0} \tag{3}$$

where q_e is the amount of metal adsorbed at equilibrium (mg/g), C_e the equilibrium concentration of the adsorbate (mg/L), and Q^0 (mg/g) and b (L/mg) are the Langmuir constants related to the adsorption capacity and energy of adsorption, respectively.

The Freundlich model assumes adsorption on heterogeneous surfaces. The linear form of the Freundlich isotherm equation is represented as follows:

$$\log q_e = \log K_F + \frac{1}{n} \log C_e \tag{4}$$

where K_F is the adsorption equilibrium constant relating to the adsorbent capacity, and $1/n$ is the parameter relating the adsorption intensity.

The Temkin isotherm is based on the interaction between adsorbate and adsorbent, which causes heat of adsorption due to repulsions forces. The linear form of the Temkin equation is given by the following equation:

$$q_e = B \ln (K_T) + B \ln (C_e) \tag{5}$$

and $B = \frac{RT}{b_T}$

where K_T (L/g) and B (J/mol) are the Temkin and heat constants of sorption, respectively. R = universal gas constant (8.314 J/mol/K), and T = Temperature at 298 K.

The Langmuir, Freundlich, and Temkin isotherm parameters for the adsorption of lead (II) onto G-26 and MTS9570 resins were calculated by using isotherms and their correlation coefficients and listed in Table 2. Comparison of the correlation coefficients values shows that the adsorption of Pb(II) onto G-26 and MTS9570 resins is fitted better by Langmuir model ($R^2 = 0.9973$ – 0.9906) and Freundlich than Temkin models ($R^2 = 0.9806$ – 0.9943 and $R^2 = 0.9681$ – 0.9557). The Langmuir, Freundlich, and Temkin isotherms of the adsorption of Pb (II) on G-26 and MTS9570 are presented in Figures 8–10, respectively.

Table 2. The isotherm parameters for Pb(II) adsorption on G-26 and MTS9570.

	G-26	MTS9570
Langmuir isotherm		
Q^0 (mg/g)	45.45	38.46
b (L/mg)	0.082	0.221
R^2	0.9973	0.9906
Freundlich isotherm		
K_F (mg/g)	19.16	20.52
n	5.740	7.450
R^2	0.9896	0.9960
Temkin isotherm		
b_T	294.9	669.6
B	8.40	3.70
R^2	0.9681	0.9557

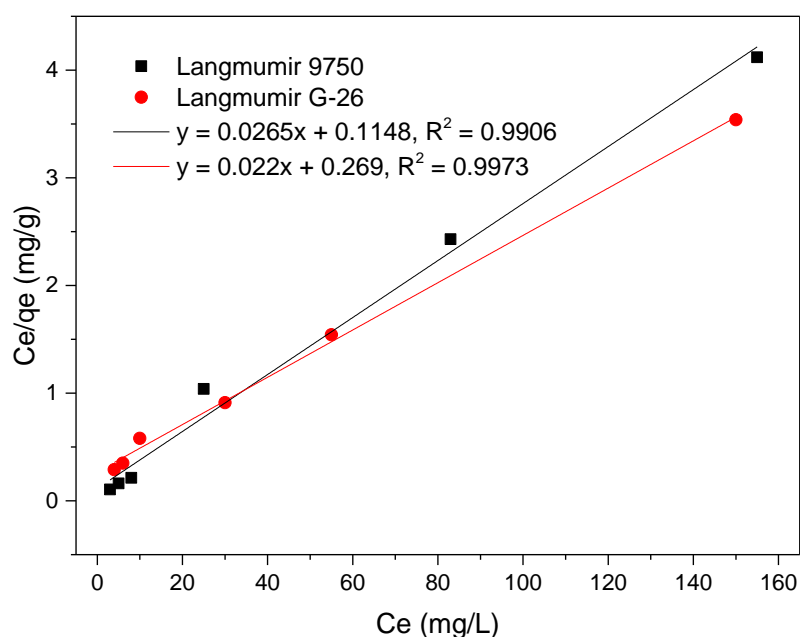


Figure 8. Langmuir isotherm of Pb(II) adsorption on G-26 and MTS9570.

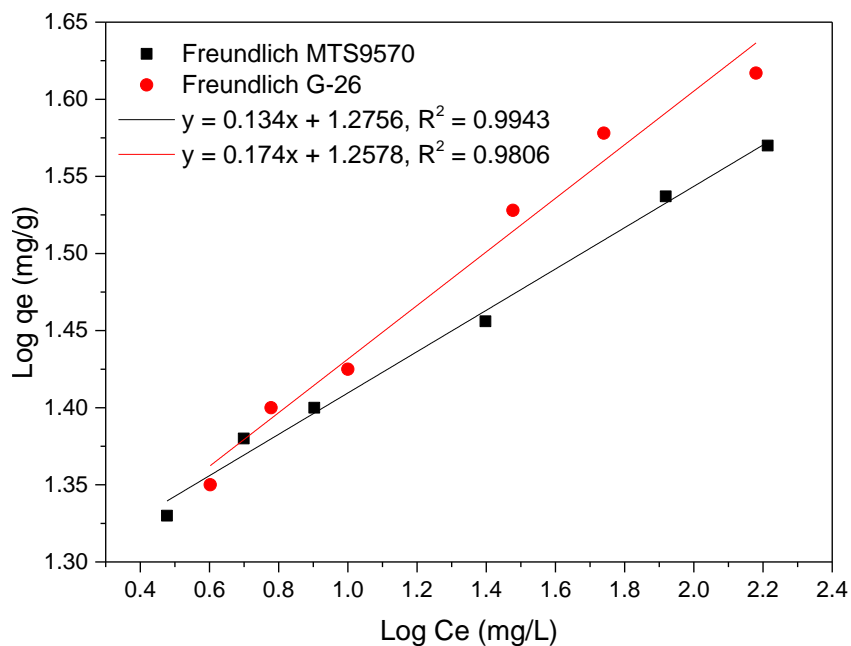


Figure 9. Freundlich isotherm of Pb(II) adsorption on G-26 and MTS9570.

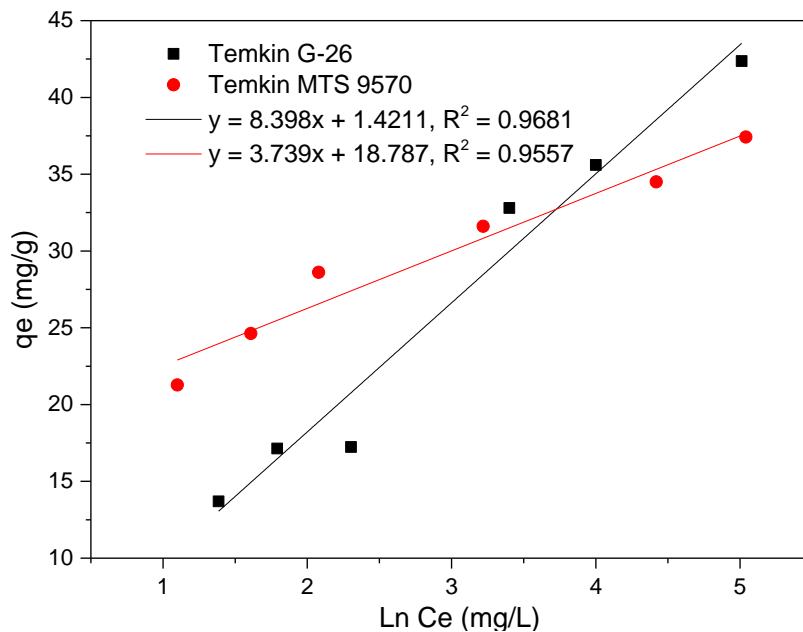


Figure 10. Temkin isotherm of Pb(II) adsorption on G-26 and MTS9570.

The maximum adsorption capacities of G-26 and MTS 9570 resins are excellent compared with some other adsorbents for the adsorption of Pb(II) (Table 3).

Table 3. Comparison of maximum adsorption capacity of G-26 and MTS 9570 resins with some other adsorbents for adsorption of Pb(II).

Adsorbent	Sorption Capacity for Cu (II) (mg/g)	Conditions	References
SBA-15	41.50	pH = 2.5–4, 30 °C	[29]
MWCNT	17.54	pH = 6.5, 20 °C	[31]
APTS-SBA-15-AB	43.50	pH = 6.0, 60 °C	[38]
MCCM	45.50	pH = 6.0, 30 °C	[39]
1,8-DAN/XAD-4	29.01	pH = 6.0–7.0, 20 °C	[40]
Copolymer 2-hydroxyethyl methacrylate	31.50	pH = 6.0–7.0, 20 °C	[41]
Crosslinked chitosan with epichlorohydrin	34.13	pH = 7.0, NA	[42]
Purolite C100	9.64	pH = NA, 25 °C	[43]
Amberlite XAD-2 functionalized with Tiron	12.60	pH = 4.0–5.5, 25 °C	[44]
Purolite A830	30.61	pH = 7.0–9.0, 50 °C	[45]
Bentonite	28.00	pH = 6.0–9.0, 25 °C	[46]
Zeolite	24.40	pH = 9.0, 20 °C	[47]
G-26	45.45	pH = 3.5, 20 °C	This work
MTS9570	38.46	pH = 3.5, 20 °C	This work

3.8. Adsorption Kinetics

The kinetics for the adsorption of Pb(II) onto G-26 and MTS9570 resins were investigated using Lagergren pseudo-first-order and pseudo-second-order models, represented by Equations (6) and (7), respectively [48,49].

$$\ln(q_e - q_t) = \ln(q_e) - \frac{k_1 t}{2.303} \quad (6)$$

where q_t and q_e are the amounts of metal ions adsorbed (mg/g) at equilibrium and at contact time t (min), respectively; k_1 (min^{-1}) is the first-order rate constant. The plots of $\ln(q_e - q_t)$ versus t are presented in Figure 11, and the rate constants (k_1) are listed in Table 4.

$$\frac{t}{q_e} = \frac{t}{q_e} + \frac{1}{k_2 q_e^2} \quad (7)$$

where k_2 (g/mg/min) is the rate constant of pseudo-second-order adsorption. The plots of $\frac{t}{q_t}$ versus t are shown in Figure 12, and the rate constants (k_2) are presented in Table 4. Pseudo-first-order and pseudo-second-order parameters are listed in Table 4. The results clearly show that R^2 values of the second-order kinetic model for both resins are closer to 1 than the results obtained from the first-order kinetic model. Therefore, the adsorption behavior of Pb(II) onto the resins fits the second-order kinetics. G-26 and MTS9570 resins have about the same order of magnitude for the adsorption rates even if they are characterized by different functional groups.

Table 4. Kinetic parameters for the adsorption of Pb(II) ions onto G-26 and MTS9570.

	G-26	MTS9570
Equations		
Pseudo-first-order		
q_e , exp (mg/g)	41.80	42.00
q_e , cal (mg/g)	3.49	2.513
k_1 (min^{-1})	−0.00017	−0.00020
R^2	0.7243	0.9090
Pseudo-second-order		
q_e , cal (mg/g)	42.50	42.10
k_2 (g/mg min)	0.00896	0.0362
R^2	0.9994	0.9999

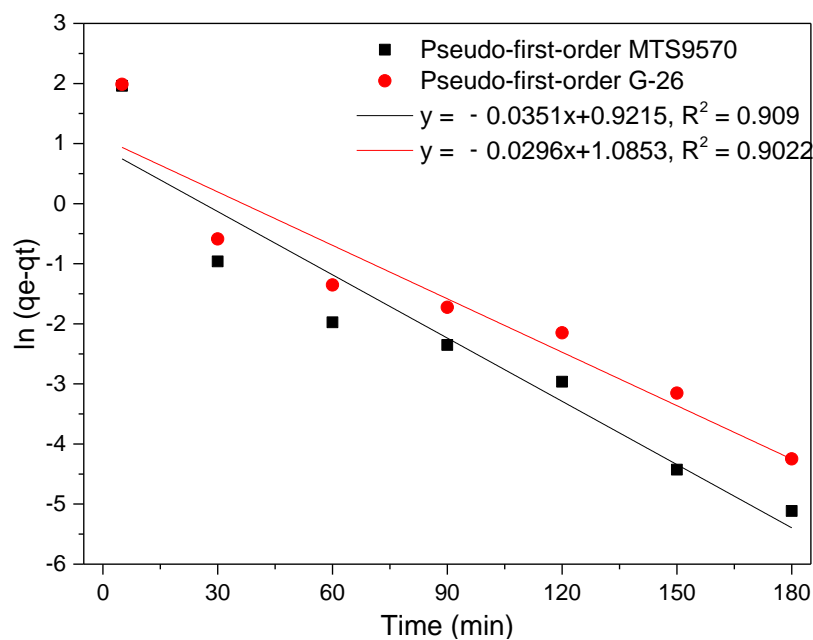


Figure 11. Pseudo-first-order modelling for adsorption of Pb(II) onto G-26 and MTS9570 resins.

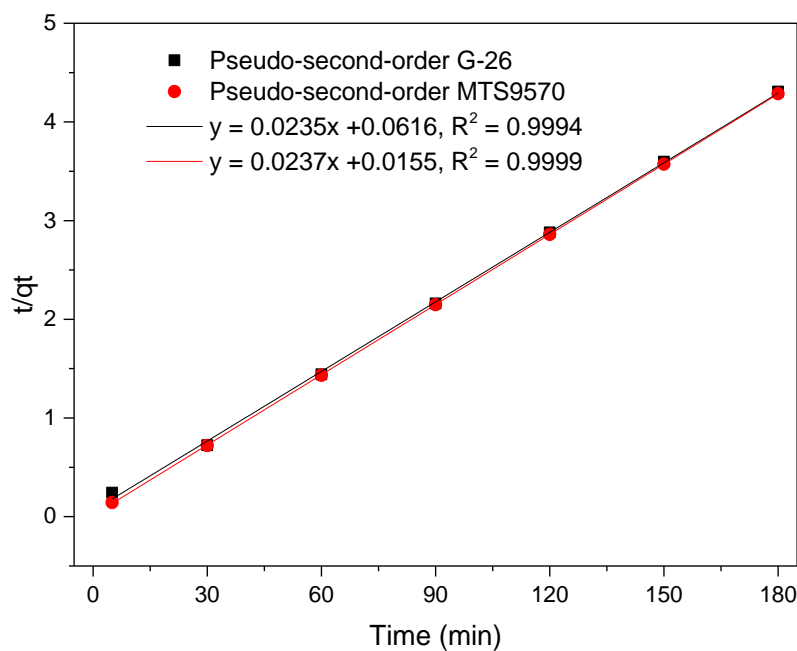


Figure 12. Pseudo-second-order modelling for adsorption of Pb(II) onto G-26 and MTS9570 resins.

3.9. Thermodynamic Evaluation of the Process

Thermodynamic parameters such as standard free energy change (ΔG°), standard enthalpy change (ΔH°), and standard entropy change (ΔS°) are very important for analyzing the nature of an ion-exchange process [50]. To estimate these parameters, the influence of temperature on the adsorption process was studied.

The thermodynamic parameters, including ΔG° , ΔH° , and ΔS° , were determined using the following equations:

$$\Delta G^\circ = -RT \ln K, K = \frac{q_e}{C_e} \tag{8}$$

$$\Delta G^\circ = \Delta H^\circ - T \Delta S^\circ \tag{9}$$

or

$$\ln K = -\frac{\Delta H^\circ}{RT} + \frac{\Delta S^\circ}{R} \quad (10)$$

where K is the the distribution coefficient calculated from the Langmuir equation, R is the universal gas constant (8.314 J/mol/K), and T is absolute temperature (K). The values of ΔH° and ΔS° could be obtained from the slope and intercept of the linear plot between $\ln K$ versus $1/T$. The calculated values of thermodynamic parameters are listed in Table 5.

Table 5. Thermodynamic parameters for the adsorption of Pb(II) on G-26 and MTS9570.

Resin	ΔG (kJ/mol)				ΔH (kJ/mol)	ΔS (kJ/mol)	R^2
	293 K	303 K	313 K	353 K			
G-26	−38.34	−40.96	−43.58	−46.20	42.30	131.30	0.9642
MTS9570	−27.93	−29.73	−31.60	−33.50	32.07	95.44	0.9266

The negative values for free energy change ΔG° confirm the feasibility and spontaneous process for Pb (II) adsorption onto both resins, and the positive values of ΔH° (42.3 and 32.07 kJ/mol for G-26 and MTS9570, respectively) indicate the endothermic nature of the adsorption process. The higher value of $T\Delta S$ than ΔH suggests that the adsorption process is enthalpy-driven [51].

3.10. Desorption Studies

The recyclability of the sorbent is one of the most important factors in wastewater treatment [52]. In this work, the regeneration and reuse of the ion exchangers were investigated. For the elution of Pb from G-26 and MTS9570 resins, various electrolytes volumes of HCl, HNO₃, CH₃COOH, and C₂H₂O₄ were tested at room temperature. It was observed that the best elution result was obtained using 40 mL volume of HCl with 15% (*v/v*) concentration and 20 min of elution time for the 0.5 g loaded resin, as shown in Figure 13.

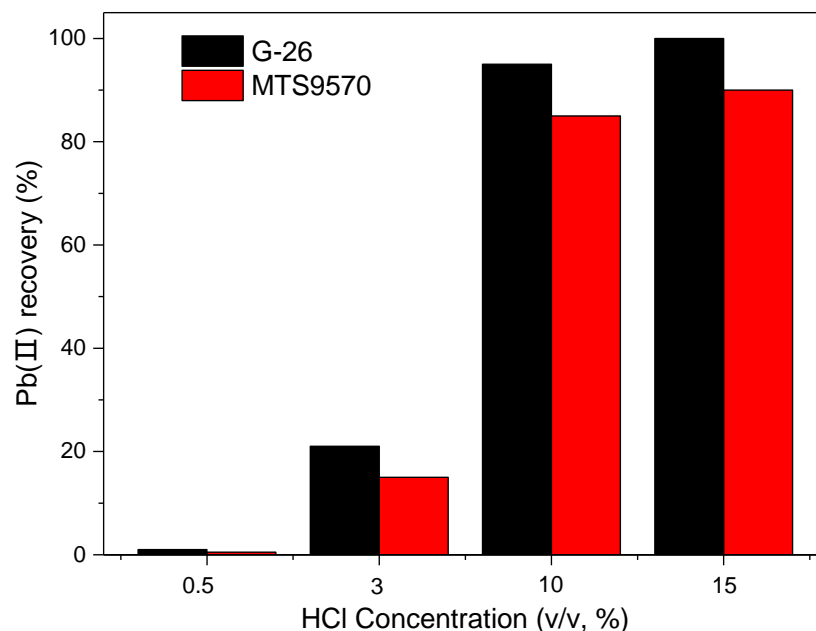


Figure 13. Elution of G-26 and MTS9570 at different HCL concentrations (*v/v*) at 0.5 g of resin dosage, 20 min agitation time, 40 mL volume, and at room temperature.

The adsorption-desorption cycle was repeated three times using the same resin, and the results are presented in Table 6.

Table 6. Adsorption and desorption cycles of Pb(II) on G-26 and MTS9570 resins.

Resin	Pb(II) Removal %			Pb(II) Recovery %		
	Adsorption Cycle			Elution Cycle		
	First Adsorption	Second Adsorption	Third Adsorption	First Elution	Second Elution	Third Elution
G-26	100	100	100	100	100	100
MTS9570	100	97	96	90	86	76

Table 6 shows excellent stability of G-26 resin in all the three cycles, with 100% for adsorption and 100% for elution of Pb(II) ions. While, for the MTS9570 resin, the adsorption percentage was 100, 97, and 96 in the first cycle, second cycle, and third cycle, respectively, the elution efficiency was 90%, 86%, and 76% in the first cycle, second cycle, and third cycle, respectively. This result agrees with the earlier results of Volesky [53]. The performance degradation of MTS9570 resin might be due to its macroporous S-DVB structure (low surface area) and negative swelling factor (−5%) as well. Swelling is an important parameter for the completion of adsorption reaction [54]. Negative swelling factor means volume shrink, which leads to specific surface area adsorption-site decrease.

4. Conclusions

This work presents an investigation on the performance of G-26 and MTS9570 resins for the adsorption of lead ions from synthesized wastewater. The resin dosage, pH of solution, contact time, initial metal concentration, and temperature were the main operation parameters that affected the adsorption of Pb(II). For all the systems studied, the pseudo-second-order chemical reaction kinetics provided the best correlation of the experimental data for both resins. The Langmuir model better described the adsorption equilibrium. The maximum adsorption capacities to Pb(II) were 45.45 and 38.46 mg/g for G-26 and MTS9570, respectively. The negative value of free energy ΔG° and the positive value of ΔH° obtained indicate that the adsorption process is spontaneous and endothermic in nature. The resin recycling study shows that the most efficient Pb(II) desorption for both resins was obtained using 40 mL volume of HCl with 15% (*v/v*) concentration and 20 min of elution time at room temperature. Results of consecutive adsorption/desorption studies show that G-26 resin exhibited excellent stability in all the three cycles, with 100% recovery for adsorption and 100% efficiency for elution of Pb(II) ions. Furthermore for the MTS9570 resin, its performance degradation might be due to its macroporous S-DVB structure (low surface area) and negative swelling factor. Gel-structure resin G-26 is more effective than macroporous-structure resin (MTS9570) for the removal/recovery of lead ions from wastewater.

Author Contributions: All authors contributed to the study conception and design. Material preparation, data collection, and analysis were performed by S.E., Q.S., A.M., L.A.J. and Y.Z.; the first draft of the manuscript was written by S.E. and Y.Z. All authors commented on previous versions of the manuscript. All authors have read and agreed to the published version of the manuscript.

Funding: Discovery Program Grant # RGPIN/004354-2017, Natural Sciences and Engineering Research Council of Canada (NSERC).

Data Availability Statement: The datasets generated during the current study are available from the corresponding author on reasonable request.

Acknowledgments: The authors gratefully acknowledge the financial support of this work by the Natural Sciences and Engineering Research Council of Canada (NSERC) and Markus Wälle in the Core Research Equipment and Instrument Training Network (CREAIT) at Memorial University of Newfoundland for metal concentration analysis.

Conflicts of Interest: The authors have no relevant financial or non-financial interests to disclose.

References

1. Zhang, Y.H. 100 years of Pb deposition and transport in soils in Champaign, Illinois, USA. *Water Air Soil Pollut.* **2003**, *146*, 197–210. [[CrossRef](#)]
2. Selvi, A.; Rajasekar, A.; Theerthagiri, J.; Ananthaselvam, A.; Sathishkumar, K.; Madhavan, J.; Rahman, P. Integrated remediation processes toward heavy metal removal/recovery from various environments—A review. *Front. Environ. Sci.* **2019**, *7*, 66. [[CrossRef](#)]
3. Ahuja, S.; Loganathan, B.G. (Eds.) *Contaminants in Our Water: Identification and Remediation Methods*; American Chemical Society: Washington, DC, USA, 2020.
4. Qasem, N.A.A.; Mohammed, R.H.; Lawal, D.U. Removal of heavy metal ions from wastewater: A comprehensive and critical review. *NPJ Clean Water* **2021**, *4*, 36. [[CrossRef](#)]
5. Rahman, M.L.; Sarjadi, M.S.; Guerin, S.; Sarkar, S.M. Poly (amidoxime) Resins for Efficient and Eco-friendly Metal Extraction. *ACS Appl. Polym. Mater.* **2022**, *4*, 2216–2232. [[CrossRef](#)]
6. Sunder, G.S.S.; Rohanifar, A.; Alipourasiabi, N.; Lawrence, J.G.; Kirchoff, J.R. Synthesis and Characterization of Poly(pyrrole-1-carboxylic acid) for Preconcentration and Determination of Rare Earth Elements and Heavy Metals in Water Matrices. *ACS Appl. Mater. Interfaces* **2021**, *13*, 34782–34792. [[CrossRef](#)]
7. Chu, F.X.; Liu, C.; Wu, H.; Liu, X. Advances in Chelating Resins for Adsorption of Heavy Metal Ions. *Ind. Eng. Chem. Res.* **2022**, *61*, 11309–11328. [[CrossRef](#)]
8. Chen, T.; Li, H.; Wang, H.; Zou, X.; Liu, H.; Chen, D.; Zhou, Y. Removal of Pb(II) from Aqueous Solutions by Periclase/Calcite Nanocomposites. *Water. Air Soil Pollut.* **2019**, *230*, 299–314. [[CrossRef](#)]
9. Lalmi, A.; Bouhidel, K.-E.; Sahraoui, B.; Anfif, C.E.H. Removal of lead from polluted waters using ion exchange resin with Ca(NO₃)₂ for elution. *Hydrometallurgy* **2018**, *178*, 287–293. [[CrossRef](#)]
10. Wang, N.; Bora, M.; Song, H.; Tao, K.; Wu, J.; Hu, L.; Liao, J.; Lin, S.; Triantafyllou, M.S.; Li, X. Hyaluronic Acid Methacrylate Hydrogel-Modified Electrochemical Device for Adsorptive Removal of Lead(II). *Biosensors* **2022**, *12*, 714. [[CrossRef](#)]
11. Ren, H.; Li, B.; Neckenig, M.; Wu, D.; Li, Y.; Ma, Y.; Li, X.; Zhang, N. Efficient lead ion removal from water by a novel chitosan gel-based sorbent modified with glutamic acid ionic liquid. *Carbohydr. Polym.* **2019**, *207*, 737–746. [[CrossRef](#)]
12. World Health Organization. *Guideline for Drinking-Water Quality*, 4th ed.; World Health Organization: Geneva, Switzerland, 2017.
13. Sunder, G.S.S.; Adhikari, S.; Rohanifar, A.; Poudel, A.; Kirchoff, J.R. Evolution of environmentally friendly strategies for metal extraction. *Separations* **2020**, *7*, 4. [[CrossRef](#)]
14. Elfeghe, S.; Sheng, Q.; Zhang, Y. Separation of Lead and Copper Ions in Acidic Media Using an Ion-Exchange Resin with a Thiourea Functional Group. *ACS Omega* **2022**, *7*, 13042–13049. [[CrossRef](#)] [[PubMed](#)]
15. Acharya, J.; Sahu, J.N.; Mohanty, J.R.; Meikap, B.C. Removal of lead (II) from wastewater by activated carbon developed from tamarind wood by zinc chloride activation. *Chem. Eng. J.* **2009**, *149*, 249–262. [[CrossRef](#)]
16. Abou-Shady, A.; Peng, C.; Bi, J.; Xu, H.; Almeria, O.J. Recovery of Pb (II) and removal of NO₃⁻ from aqueous solutions using integrated electrodialysis electrolysis, and adsorption process. *Desalination* **2012**, *286*, 304–315. [[CrossRef](#)]
17. Gherasim, C.V.; Krivcik, J.; Mikulasek, P. Investigation of batch electrodialysis process for removal of lead ions from aqueous solutions. *Chem. Eng. J.* **2014**, *256*, 324–334. [[CrossRef](#)]
18. Bessel, C.A.; Laubernds, K.; Rodriguez, N.M.; Baker, R.T.K. Graphite nanofibers as an electrode for fuel cell applications. *J. Phys. Chem. B* **2001**, *105*, 1115–1118. [[CrossRef](#)]
19. Rohanifar, A.; Alipourasiabi, N.; Shyam Sunder, G.S.; Lawrence, J.G.; Kirchoff, J.R. Reversible chelating polymer for determination of heavy metals by dispersive micro solid-phase extraction with ICP-MS. *Mikrochim. Acta* **2020**, *187*, 339. [[CrossRef](#)] [[PubMed](#)]
20. Marañón, E.; Fernández, Y.; Castrillón, L. Ion exchange treatment of rinse water generated in the galvanizing process. *Water Environ. Res.* **2005**, *77*, 3054–3058. [[CrossRef](#)]
21. Pehlivan, E.; Altun, T. The study of various parameters affecting the ion exchange of Cu²⁺, Zn²⁺, Ni²⁺, Cd²⁺, and Pb²⁺ from aqueous solution on Dowex 50W synthetic resin. *J. Hazard. Mater. B* **2006**, *134*, 149–156. [[CrossRef](#)] [[PubMed](#)]
22. Cavaco, S.A.; Fernandes, S.; Quina, M.M.; Ferreira, L.M. Removal of chromium from electroplating industry effluents by ion exchange resins. *J. Hazard. Mater.* **2007**, *144*, 634–638. [[CrossRef](#)]
23. Silva, R.M.P.; Manso, J.P.H.; Rodrigues, J.R.C.; Lagoa, R.J.L. Comparative study of alginate beads and an ion exchange resin for the removal of heavy metals from a metal plating effluent. *J. Environ. Sci. Health A* **2008**, *43*, 1311–1317. [[CrossRef](#)] [[PubMed](#)]
24. Qian, J.; Zeng, Z.; Xue, W.; Guo, Q. Lead removal from aqueous solutions by 732 cation-exchange resin. *Can. J. Chem. Eng.* **2016**, *94*, 142–150. [[CrossRef](#)]
25. Guo, H.; Ren, Y.; Sun, X.; Xu, Y. Removal of Pb²⁺ from aqueous solutions by a high-efficiency resin. *Appl. Surf. Sci.* **2013**, *283*, 660–667. [[CrossRef](#)]
26. Tabatabaei, S.H.; Asemanrafat, M.; Nousahdi, M. Removal of Lead from aqueous phase using Amberlite and natural Zeolite. *E3S Web Conf.* **2013**, *1*, 13010. [[CrossRef](#)]
27. Vergili, I. Sorption of Pb (II) from battery industry wastewater using a weak acid cation exchange resin. *Process Saf. Environ. Prot.* **2017**, *107*, 498–507. [[CrossRef](#)]
28. Xiong, C.; Yao, C. Adsorption behavior of gel-type weak acid resin (110-H) for Pb²⁺. *Trans. Nonferr. Met. Soc. China* **2008**, *18*, 1290–1294. [[CrossRef](#)]

29. Thu, P.T.T.; Thanh, T.T.; Phi, H.N.; Kim, S.J.; Vo, V. Adsorption of lead from water by thiol-functionalized SBA-15 silicas. *J. Mater. Sci.* **2010**, *45*, 2952–2957. [[CrossRef](#)]
30. Merganpour, A.M.; Nekuonam, G.; Tomaj, O.A.; Kor, Y.; Safari, H. Efficiency of lead removal from drinking water using cationic resin Purolite. *Environ. Health Eng. Manag. J.* **2015**, *2*, 41–45.
31. Ren, X.M.; Shao, D.D.; Yang, S.T.; Hu, J.; Sheng, G.D.; Tan, X.L.; Wang, X.K. Comparative study of Pb(II) sorption on XC-72 carbon and multi-walled carbon nanotubes from aqueous solutions. *Chem. Eng. J.* **2011**, *170*, 170–177. [[CrossRef](#)]
32. Elfeghe, S.; Anwar, S.; Zhang, Y. Adsorption and removal studies of cadmium ion onto sulfonic/phosphonic acid functionalization resins. *Can. J. Chem. Eng.* **2022**, *100*, 3006–3014. [[CrossRef](#)]
33. Zhang, Y.; Elfeghe, S.; Tang, Z.D. Mechanism study of Cd(II) ion adsorption onto resins with sulfonic/phosphonic groups using electronic structure methods. *J. Mol. Liq.* **2022**, *358*, 119199. [[CrossRef](#)]
34. Al-Anber, M.; Al-Anber, Z.A. Utilization of natural zeolite as ion-exchange and sorbent material in the removal of iron. *Desalination* **2007**, *225*, 70–81. [[CrossRef](#)]
35. Langmuir, I. The Constitution and Fundamental Properties of Solids and Liquids. *Part I Solids J. Am. Chem. Soc.* **1916**, *38*, 2221–2295. [[CrossRef](#)]
36. Freundlich, H.M.F. Über die Adsorption in Lösungen. *Z. Phys. Chem.* **1906**, *57*, 385–470. [[CrossRef](#)]
37. Temkin, M.; Pyzhev, V. Kinetics of Ammonia Synthesis on Promoted Iron Catalysts. *Acta Physicochim. URSS* **1940**, *12*, 327–356.
38. Da'na, E.; Sayari, A. Adsorption of heavy metals on amine-functionalized SBA-15 prepared by co-condensation: Applications to real water samples. *Desalination* **2012**, *285*, 62–67. [[CrossRef](#)]
39. Luo, X.; Zeng, J.; Liu, S.; Zhang, L. An effective and recyclable adsorbent for the removal of heavy metal ions from aqueous system: Magnetic chitosan/cellulose microspheres. *Bioresour. Technol.* **2015**, *194*, 403–406. [[CrossRef](#)]
40. Hoque, M.I.U.; Chowdhury, D.A.; Holze, R.; Chowdhury, A.N.; Azam, M.S. Modification of Amberlite XAD-4 resin with 1,8-diaminonaphthalene for solid phase extraction of copper, cadmium and lead, and its application to determination of these metals in dairy cow's milk. *J. Environ. Chem. Eng.* **2015**, *3*, 831–842. [[CrossRef](#)]
41. Moradi, O.; Aghaie, M.; Zare, K.; Monajjemi, M.; Aghaie, H. The study of adsorption characteristics Cu²⁺ and Pb²⁺ ions onto PHEMA and P(MMA-HEMA) surfaces from aqueous single solution. *J. Hazard. Mater.* **2009**, *170*, 673–679. [[CrossRef](#)]
42. Chen, A.H.; Liu, S.C.; Chen, C.Y. Comparative adsorption of Cu(II), Zn(II), and Pb(II) ions in aqueous solution on the crosslinked chitosan with epichlorohydrin. *J. Hazard. Mater.* **2008**, *154*, 184–191. [[CrossRef](#)]
43. Abo-Farha, S.A.; Abdel-Aal, A.Y.; Ashour, I.A.; Garamon, S.E. Removal of some heavy metal cations by synthetic resin purolite C100. *J. Hazard. Mater.* **2009**, *169*, 190–194. [[CrossRef](#)]
44. Kumar, M.; Rathore, D.P.S.; Singh, A.K. Metal ion enrichment with Amberlite XAD-2 functionalized with Tiron: Analytical applications. *Analyst* **2000**, *125*, 1221–1226. [[CrossRef](#)]
45. Jachua, J.; Hubicki, Z. Sorption of heavy metal complexes with MGDA on the macroporous anion exchanger Purolite A830. *CHEMIK* **2013**, *67*, 693–700.
46. Futralan, C.M.; Kan, C.-C.; Dalida, M.L.; Hsien, K.-J.; Pascua, C.; Wan, M.-W. Comparative and competitive adsorption of copper, lead, and nickel using chitosan immobilized on bentonite. *Carbohydr. Polym.* **2011**, *83*, 528–536. [[CrossRef](#)]
47. Sharifipour, F.; Hojati, S.; Landi, A.; Cano, A.F. Kinetics and Thermodynamics of Lead Adsorption from Aqueous Solutions Onto Iranian Sepiolite and Zeolite. *Int. J. Environ. Res.* **2015**, *9*, 1001–1010.
48. Lagergren, S. Zur theorie der sogenannten adsorption gelöster stoffe. *K. Sven. Vetensk. Handl.* **1898**, *24*, 1–39.
49. Ho, Y.S.; McKay, G. Pseudo-second order model for sorption processes. *Process Biochem.* **1999**, *34*, 451–465. [[CrossRef](#)]
50. Ahmadi, M.; Teymouri, P.; Setodeh, A. Adsorption of Pb (II) from aqueous solution onto lewattit for 36 nano resin: Equilibrium and kinetic studies. *Environ. Eng. Manag. J.* **2011**, *10*, 1579–1587. [[CrossRef](#)]
51. An, F.Q.; Wu, R.Y.; Li, M.; Hu, T.P.; Gao, J.F.; Yuan, Z.G. Adsorption of heavy metal ions by iminodiacetic acid functionalized D301 resin: Kinetics, isotherms and thermodynamic. *React. Funct. Polym.* **2017**, *118*, 42–50. [[CrossRef](#)]
52. Burham, N. Separation and preconcentration system for lead and cadmium determination in natural samples using 2-aminoacetylthiophenol modified polyurethane foam. *Desalination* **2009**, *249*, 1199–1205. [[CrossRef](#)]
53. Volesky, B.; Weber, J.; Park, J.M. Continuous-flow metal biosorption in a regenerable Sargassum column. *Water Res.* **2003**, *37*, 297–306. [[CrossRef](#)]
54. Teixeira, V.G.; Coutinho, F.M.B.; Petrocínioa, F.R.M.; Gomesa, A.S. Determination of accessible chloromethyl groups in chloromethylated styrene-divinylbenzene copolymers. *J. Braz. Chem. Soc.* **2005**, *16*, 951–956. [[CrossRef](#)]